Available online at www.sciencedirect.com
ScienceDirect
Energy and Buildings 39 (2007) 1065–1072
ENERGY and BUILDINGS
www.elsevier.com/locate/enbuild

Numerical model and experimental validation of heat storage with phase change materials

Jacques Bony *, Stéphane Citherlet

Laboratory of Solar Energetics and Building Physics (LESBAT), Applied University of West-Switzerland (HES-SO/HEIG-VD), CH-1401 Yverdon-les-Bains, Switzerland

Received 27 June 2006; received in revised form 10 October 2006; accepted 20 October 2006

Abstract

This paper describes the numeric model developed to simulate heat transfer in phase change materials (PCM) plunged in water tank storage. This model, based on the enthalpy approach, takes into account the conduction and the convection into PCM as well as at the interface between PCM and water of the storage. Furthermore, hysterisis and subcooling are also included. This model has been implemented in an existing TRNSYS type of water tank storage. It allows the simulation of a water storage tank filled with PCM modules made of different materials and different shapes such as cylinders, plates or spheres bed. Comparisons between measurements and simulations has been undertake to evaluate the potential of this model.

Keywords: PCM; TRNSYS; Heat transfer; Latent heat; Solar energy

1. Introduction

For several decades, different numerical models of storage tanks using PCM for latent energy storage have been developed; a few of these models have been elaborated to work with the TRNSYS simulation package [1]. Unfortunately, none of them gave enough satisfaction to allow a large diffusion, either due to a lack of time to test its reliability [2], or a lack of flexibility which does not allow the modelling of different types of containers for PCM [3].

In the framework of the IEA Task 32, which investigates advanced storage solutions in thermal solar systems for buildings, the potential of new PCMs is investigated to increase the energy density of small sized water storage tanks. This approach should have the advantage of reducing solar store volume for a given solar fraction as well as the store's heat losses. It should also increase the solar fraction for a given available volume. To fulfill the Task's requirements, we have developed a numerical model and compared data measurements with simulations results.

2. Numerical model

The developed model is an extension of the existing TRNSYS Type 60, for stratified fluid tanks based on sensible energy storage only [4]. The tank can be made up to 100 fully mixed stacked volume segments (Fig. 1a). This model has been adapted to be able to take into account the PCM calculation.

The standard Type 60 includes internal heat exchangers, two direct input–output and auxiliary heaters. The water tank can be considered vertical or horizontal. This model allows the simulation of most of water storage tanks. The number of horizontal segments called also node (Fig. 1a) determines the degree of calculation accuracy that can be improved with the increase of the node number. The height and the thermal losses of every layer can be defined separately. So it is possible to take into account the losses by thermal bridge as for example a pipe junction.

Fig. 1b and Eq. (1) show the different heat fluxes of the energy balance considered in each *i*th node (segment or layer) of the water tank [4]. For each node, the temperature is assumed to be uniform.

The energy balance for each storage node is given by the following equation:

$$\dot{Q}_i^{(\text{medium})} = \dot{Q}_i^{(\text{flow})} + \dot{Q}_i^{(\text{hx})} + \dot{Q}_i^{(\text{aux})} + \dot{Q}_i^{(\text{cond})} + \dot{Q}_i^{(\text{loss})} + \dot{Q}_i^{(\text{modules})} \quad (1)$$

* Corresponding author.
E-mail address: jacques@leig-vd.ch (J. Bony).

0378-7788/$ – see front matter
doi:10.1016/j.enbuild.2006.10.017

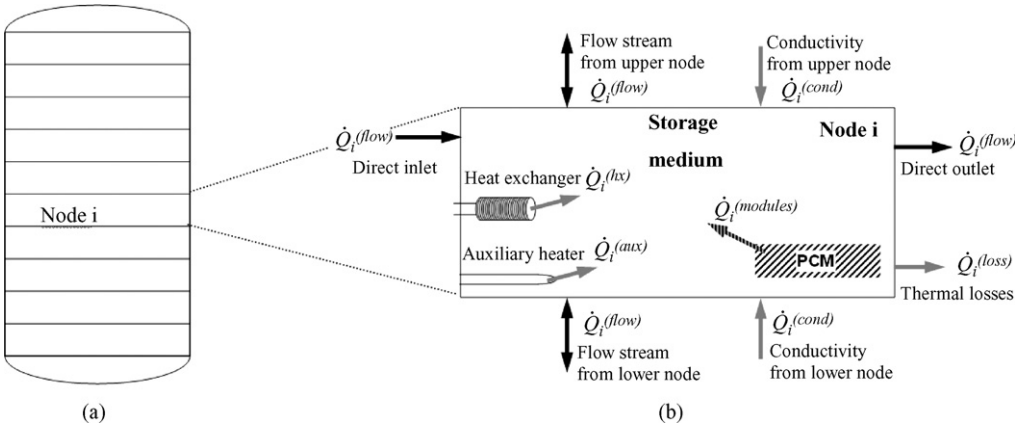

Fig. 1. Energy balance for each ith water node.

with $Q^{(\text{medium})}$ is the energy of the storage medium of node i; $Q^{(\text{flow})}$ the charging or discharging energy via direct (inlet/outlet) flow including the flow upward/downward in the tank; $Q^{(\text{hx})}$ the heat flux through internal heat exchanger; $Q^{(\text{aux})}$ the auxiliary energy; $Q^{(\text{cond})}$ the thermal conduction to neighbouring nodes; $Q^{(\text{loss})}$ the thermal losses through the tank envelope to the ambient; $Q^{(\text{modules})}$ is the energy exchange between the storage medium and PCM modules.

The energy exchange between the storage medium and the PCM modules is governed by the following equation [5]:

$$\dot{Q}_i^{(\text{modules})} = -N^{(\text{modules})}\{U_i A_i^{\text{PCM}}[T_i - T_i^{\text{PCM}}(h_i^{\text{PCM}})]\} \quad (2)$$

with $N^{(\text{modules})}$ is the number of PCM containers; U the heat transfer coefficient water/PCM; A the surface between water and PCM container; T the storage medium temperatures (node i); T^{PCM} is the surface temperatures of the PCM container.

The calculation of heat transfer through the PCM uses the enthalpy method, which means that for a given volume and a material, a continuous and reversible function can be calculated which will return the temperature T depending on the calculated enthalpy h. This temperature is used during the simulation to determine the node temperature, according to the enthalpy of the system at time t. Fig. 2 shows this function constituted of a succession of five straight lines: two for the sensible heat in solid or liquid phase and three straight lines in the phase change part. Thus, the accuracy is enough for the calculations.

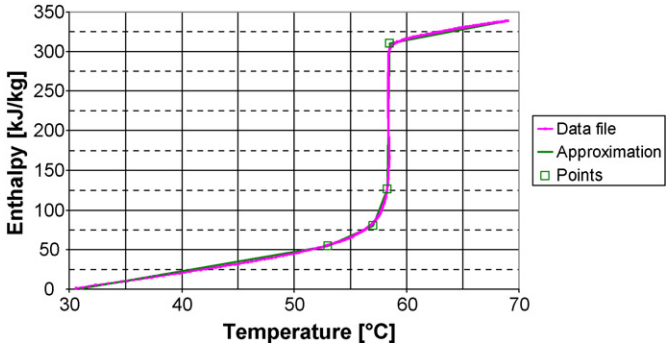

Fig. 2. Example of an enthalpy curve for a particular volume and PCM type.

2.1. Numerical approach

The numerical resolution of the set of equations can be done by an explicit or implicit method.

(A) The explicit method is simple to program but is conditionally steady. It needs to have a time step smaller than a limit value in order to avoid any divergence. On the other hand it increases simulation time.
(B) The implicit method is more complex to program but it is unconditionally steady. There is no limit for the time step except if we would like good calculation accuracy.

We have chosen the explicit method, so it is necessary to pay attention to the time step in order to avoid a calculation divergence. The criteria of convergence are calculated with the following equations [6]:

$$\text{for a surface node}: \quad Fo(2+Bi) \leq \frac{1}{2} \quad (3)$$

$$\text{for a node inside material}: \quad Fo \leq \frac{1}{4} \quad (4)$$

$$Fo = \frac{\lambda t}{\rho \,\text{Cp}\, x^2} \quad \text{and} \quad Bi = \frac{\alpha x}{\lambda} \quad (5)$$

with Fo is the Fourier number; Bi the Biot number; λ the PCM thermal conductivity (W/(m K)); t the time step simulation (s); ρ the PCM density (kg/m^3); Cp the PCM specific heat (J/(kg K)); x the distance between two nodes (m); α is the convective coefficient between water and PCM (W/(m^2 K)).

From Eqs. (6) and (7), we get the maximum time step possible for calculation. It takes into account the heat transfer coefficients (convective and conductive) as well as the thermal capacity of every node and the position of the node considered [6].

$$\text{for interface node water/PCM}, \quad t \leq \frac{\rho \,\text{Cp}\, x^2}{2\lambda(2+(\alpha x/\lambda))} \quad (6)$$

$$\text{for a node inside material}, \quad t \leq \frac{\rho \,\text{Cp}\, x^2}{4\lambda} \quad (7)$$

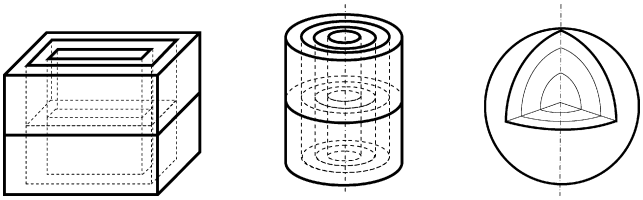

Fig. 3. Representation of different shapes available.

2.2. PCM meshing

The internal calculation model in the PCM is bi-dimensional, which allows the simulation of different PCM shapes: cylinder, sphere or plate. An onion peel approach has been used. It consists of representing a PCM element by a constant thickness layer succession whose shape depends on the object, as shown in Fig. 3.

For each node, we calculate the energy balance while supposing a uniform temperature in the volume of the corresponding node (Fig. 4), which gives an enthalpy variation given by the Eq. (8):

$$\frac{\Delta h_{i,k}^{t1}}{\Delta t} = \dot{Q}_{i,k-1\to i,k}^{t1} + \dot{Q}_{i,k+1\to i,k}^{t1} + \dot{Q}_{i-1,k\to i,k}^{t1} + \dot{Q}_{i+1,k\to i,k}^{t1} \quad (8)$$

where the heat transfer between two nodes is:

$$\dot{Q}_{i,k-1\to i,k}^{t1} = \left(\frac{\lambda_{i,k}}{x_{i,k}} + \frac{\lambda_{i,k-1}}{x_{i,k-1}}\right) A_{i,k-1\to i,k}(T_{i,k-1}^{t0} - T_{i,k}^{t0}) \quad (9)$$

with i is the vertical axe (depend of number of water nodes); k the horizontal axe (PCM meshing); λ the thermal conductivity; x the distance between two nodes; A the exchange surface between two nodes; t_0 the initial time; t_1 is the final time.

The enthalpy at t_1 time is $H_{i,k}^{t1} = H_{i,k}^{t0} + \Delta h_{i,k}^{t1}$ (10)

2.3. Hysteresis

The hysteresis phenomenon appears during cooling of materials. It results in a delay of the phase change. It does not depend on the solid phase presence in the surroundings, and therefore this process can be calculated independently for every PCM node.

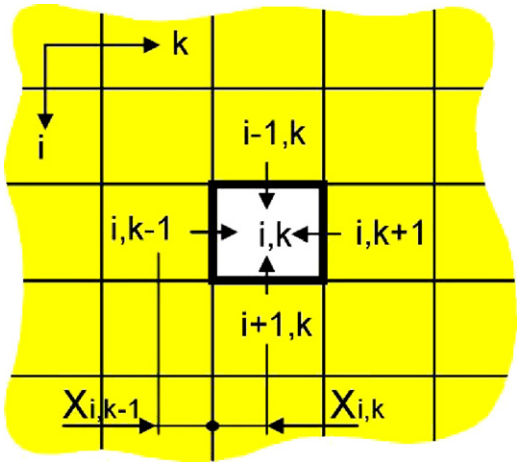

Fig. 4. PCM mesh.

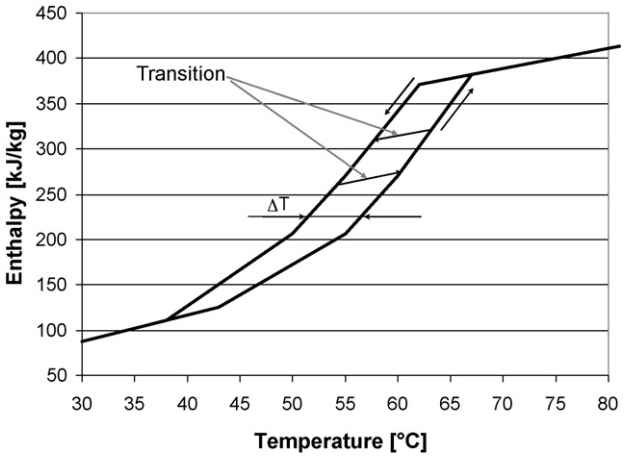

Fig. 5. Hysteresis model.

In a first time, the model did not take into account this hysteresis phenomenon and the heating or the cooling follow the same curve. Following measurements made for validation purpose, the modelisation of this physical behaviour was necessary. Fig. 5 illustrates this new function. There is a simple shift of the enthalpy curve according to a differential temperature defined with one parameter. During a heating or cooling step inside the phase change zone, the slope of transition is the same as the solid phase one in the bottom part of the phase change. It is also identical to the slope of the liquid phase in the superior part of the phase change. It avoids discontinuity of the enthalpy curve when the transition point is close to the complete phase change (liquid or solid) (Fig. 5).

2.4. Subcooling

Contrary to the previous phenomenon, the subcooling depends on solid phase presence. The determination of this process appearance takes into account the global state of the PCM module. It is necessary that the whole PCM is in liquid phase to obtain subcooling. During the cooling mode, as soon as a PCM part reaches the point of crystallization, the whole PCM will go into solid phase (full line of Fig. 6). This phenomenon can start at a lower temperature than the solidification temperature.

Thus, for cylinders or plates, the subcooling will be able to appear only one time during the cooling process. Indeed, when crystallization starts around a condensation core, the solidification step grows in the entire element at a speed that is supposed instantaneous in the numerical model (Fig. 7). In fact, it is not the case. But it is difficult to know the crystallization propagation speed in a PCM element. The following figure shows differences between the model and reality. The measurements are made on sodium acetate with graphite during the cooling process.

In the spherical module case, this phenomenon will appear at every layer of spheres. Indeed during the thermal discharge, the

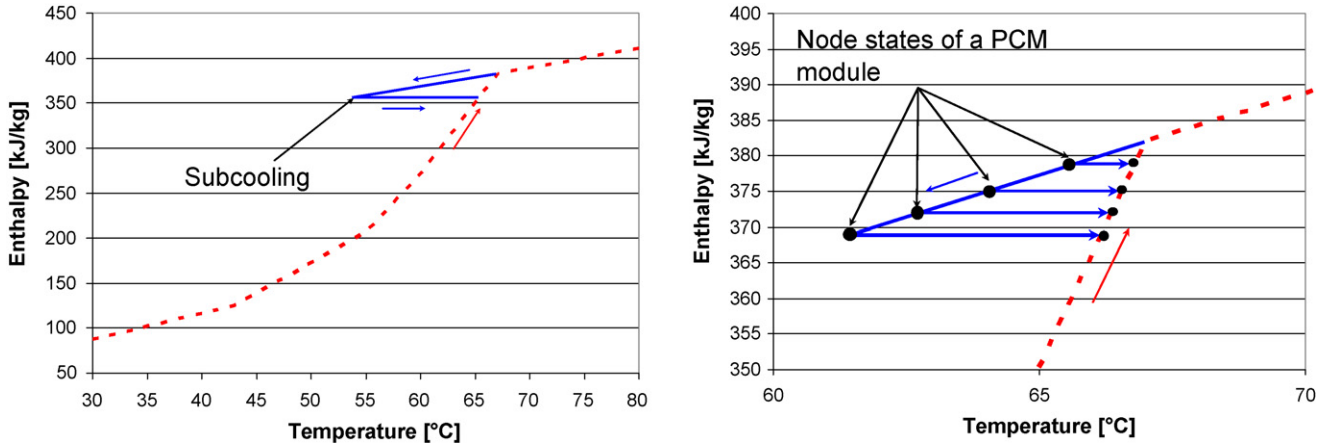

Fig. 6. Subcooling model.

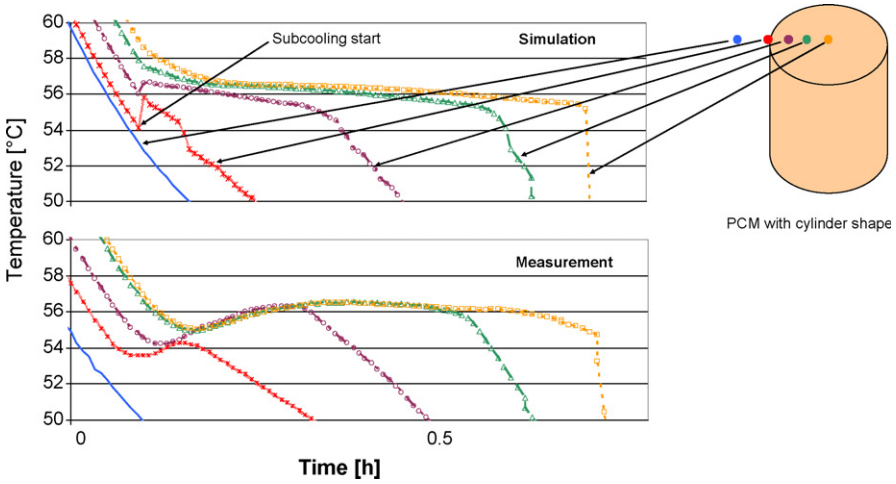

Fig. 7. Comparison between simulation and measurement about crystallization propagation speed.

lower part of the tank storage cools down in first. Thus, the first lower layer of spheres will be in subcooling process whereas the other ones should wait as the tank storage continues to cool down (Fig. 8).

The phenomena of hysteresis and subcooling can be used together as Fig. 9 shows. In the model, each of these phenomena is treated independently by a specific state indicator.

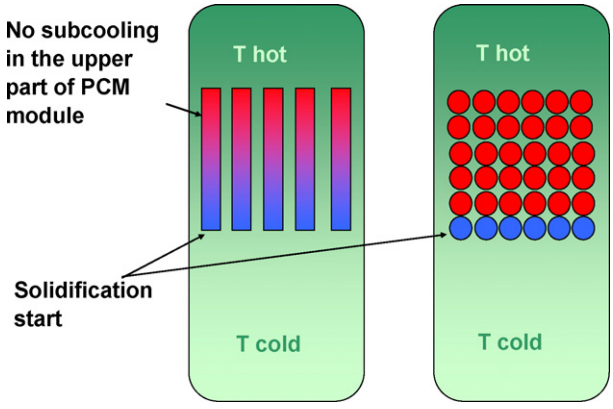

Fig. 8. Crystallization propagation process according to the container type.

2.5. Heat transfer

2.5.1. Thermal conduction inside PCM in solid or liquid phase

In order to take into account the thermal conduction difference between the solid and liquid states of a material, the model allows two distinct values for the conduction coefficient; one for the solid and one for the liquid phase.

At the time of the phase change, the thermal conductivity value is calculated by linear interpolation of the enthalpy (Fig. 10).

Below the enthalpy value H1, the thermal conductivity λ is constant and equal to λ_{sol}. Above the enthalpy value H2, the thermal conductivity is constant and is equal to λ_{liq}. Between H1 and H2, the conductivity is given by linear interpolation:

$$\lambda_{sol/liq} = \lambda_{sol} + \frac{\lambda_{liq} - \lambda_{sol}}{H2 - H1}(H^t - H1) \quad (11)$$

where, H^t is the enthalpy value at time step t and given by Eq. (10).

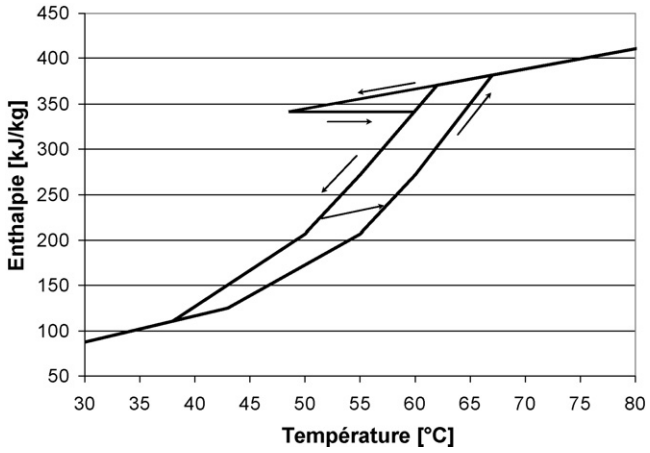

Fig. 9. Combination subcooling and hyteresis.

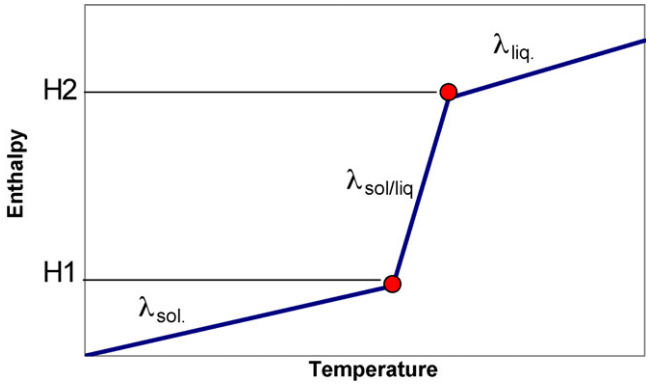

Fig. 10. Calculation of the thermal conductivity λ in accordance to the enthalpy *H*.

2.5.2. Water/PCM convection

The convective coefficient between the water of the tank storage and the PCM container is calculated for every node and each time step, according to the container shape chosen:

- Plate and cylinder → vertical plate convection [6].
- Sphere → convection around a sphere in free convection and in a sphere bed in forced convection [8].

Table 1 gives the different equations of the convective coefficient used according to the shape of the PCM module as well as the type of fluid flow around these modules [6,8].

Mixed Nusselt number and convective coefficient calculation with free and forced (water flow into tank storage) convection are given by [6]:

$$Nu_{\text{mixed}} = \left(Nu_{\text{free}}^3 + Nu_{\text{forced}}^3\right)^{1/3} \tag{12}$$

$$\alpha = \frac{Nu_{\text{mixed}}\lambda}{x}, \quad (\text{W/m}^2\,\text{K}) \tag{13}$$

2.6. Experimental data

The numerical model takes into account the hysteresis and subcooling phenomena that can be observed with some phase change materials. Although the developed model takes these two aspects into account, in the case here of paraffin, these two phenomena are negligible. So we focus on model validation of heat transfer by convection and conduction. To do this, some temperature measurements have been performed. The temperature evolution inside the PCM during the charging and discharging cycle has been monitored with thermocouples placed inside a PCM module (paraffin). The time evolution of these temperatures has been compared with the simulation.

For these measurements, we have used an aluminium container whose diameter is 88 (mm), the height 150 (mm) and the thickness 0.3 (mm). To keep a constant distance between the sensors, a grid and a cross in plastic have been used as shown in Fig. 11a.

Then the liquid paraffin is poured in the container as shown in Fig. 11b. The bottom part of the container remains open to allow sensor cables to be connected with the acquisition equipment. After the PCM has solidified, this container is plunged in the water tank with the sensor cables gone downwards (Fig. 12). This method is possible because the liquid paraffin remains in the top of the container for the following reasons:

- The density of solid and liquid paraffin is lower than that of water.
- The paraffin is non miscible with water.
- No high velocity of water flow inside the tank.

2.7. Measurements versus simulations

A first step has consisted to compare the data measurements and the simulation results done with a model which did not take into account the convection inside PCM module. In this case, the temperature measurements done in the PCM module are

Table 1
Equations for water/PCM convection

Convection	Vertical plate of cylinder	Sphere bed
Laminar free Turbulent free	$Nu = \left\{0.825 + \frac{0.387\,Ra^{1/6}}{\left[1+(0.492/Pr)^{9/16}\right]^{8/27}}\right\}^2$	$Nu = 2 + 0.56\left(\frac{Pr}{0.846+Pr}Ra\right)^{1/4}, \quad (Ra < 10^{11})$
Laminar forced Turbulent forced	$Nu_x = 0.332\,Re_x^{1/2}\,Pr^{1/3}, \quad (Re < 5.10^5)$ $Nu_x = 0.0296\,Re_x^{4/5}\,Pr^{1/3}, \quad (5.10^5 < Re < 10^7)$	$Nu_{\text{laminar}} = 0.664\left(\frac{Re}{\varepsilon}\right)^{1/2}\text{Pr}^{1/3}$, $Nu_{\text{turbulent}} = \frac{0.037(Re/\varepsilon)^{0.8}\,Pr}{1+2.443(Re/\varepsilon)^{-0.1}(Pr^{2/3}-1)}$, $Nu_{\text{global}} = 2 + \left(Nu_{\text{luminar}}^2 + Nu_{\text{turbulent}}^2\right)^{1/2}$, $Nu = (1 + 1.5(1-\varepsilon))Nu_{\text{global}}$, ($\varepsilon$ = void fraction in sphere bed)

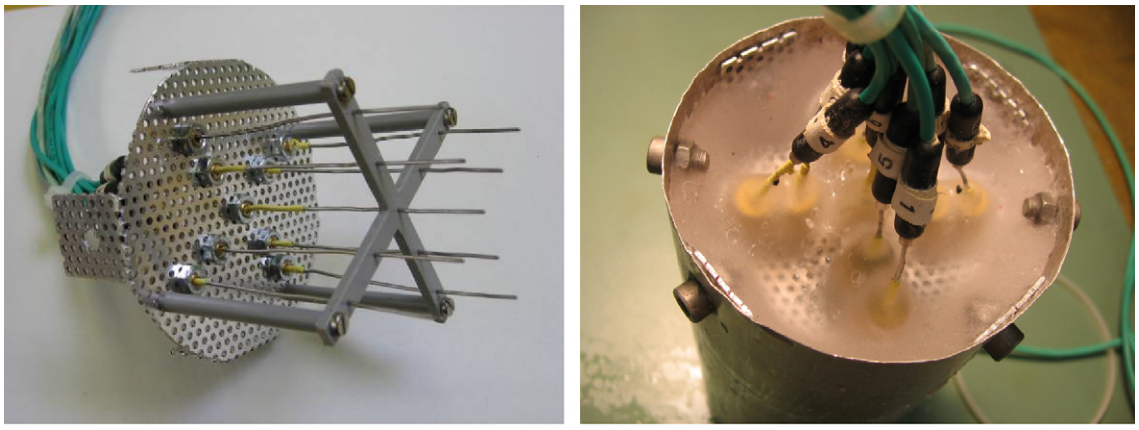

(a) (b)

Fig. 11. Temperature measurement device into paraffin. (a) Support for thermocouples. (b) Aluminium container.

very different to the results obtained by simulation, as the comparison between Figs. 13 and 14 shows. We can notice that the phase change is complete after 8 h in this simulation instead of about 3.5 h for the measurements.

2.7.1. Convection heat transfer

In order to improve the modelling of the heat transfer into the PCM module, we introduced an effective thermal conductivity which supports the convection in liquid phase of the PCM. It is given by:

$$\lambda_{\text{effective}} = \lambda\, Nu \tag{14}$$

where Nu is the Nusselt number for internal convection.

Two different equations describing the convection inside cavity have been compared manually [6,7]. As the results are similar, we have implemented the easiest equations in the model (Eqs. (15) and (16)). These two equations do not use height notion for the convective cell, which simplifies its implementation in the code. Indeed, they require only the thickness of the PCM's liquid layer to determine the Nusselt number at each node. Besides, during a thermal cycle, it is possible to have several liquid layers separated by a solid PCM layer.

The calculation of Nusselt number is given by:

◦ To a rectangular cavity with: $10^6 < Ra_L < 10^9$ [6]

$$Nu_L = 0.046\, Ra_L^{1/3} \tag{15}$$

Fig. 12. PCM container plunged in a water tank.

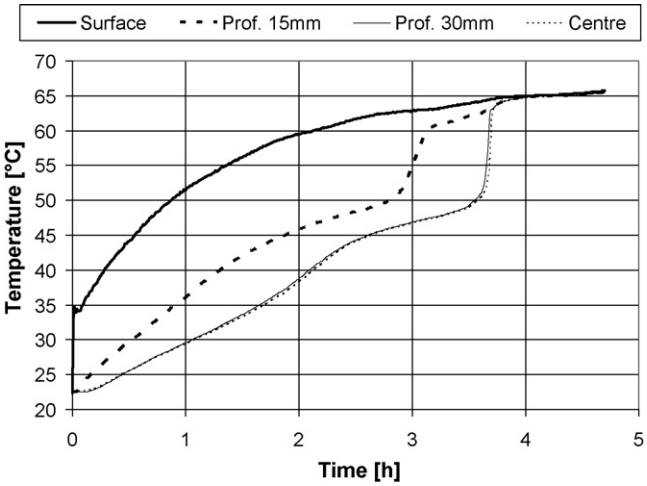

Fig. 13. Laboratory measurements.

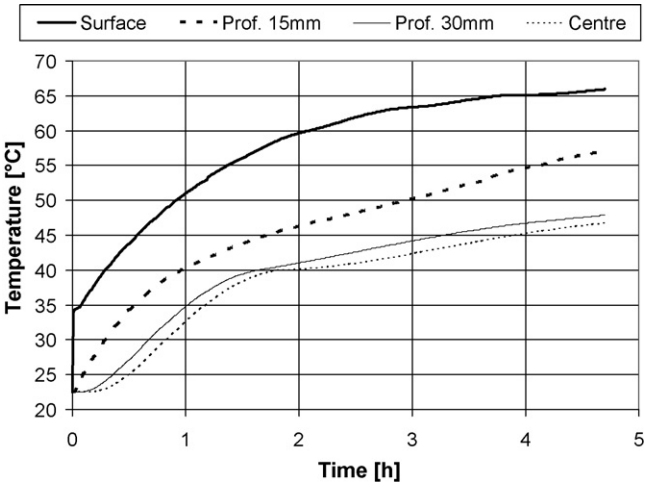

Fig. 14. Simulation without convection inside PCM.

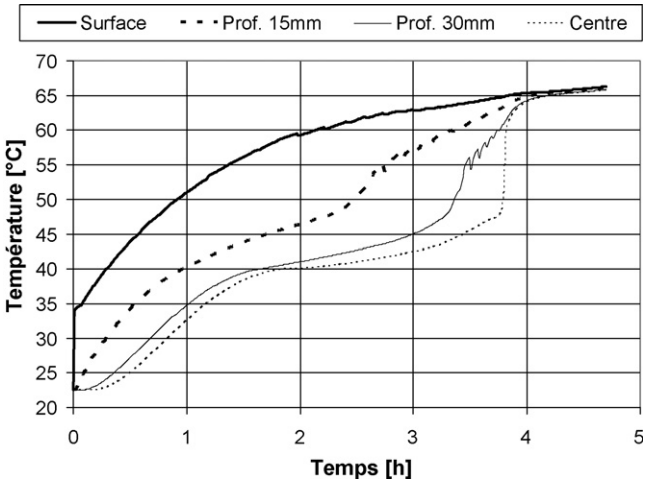

Fig. 15. Simulation taking into account internal convection inside PCM (20 nodes).

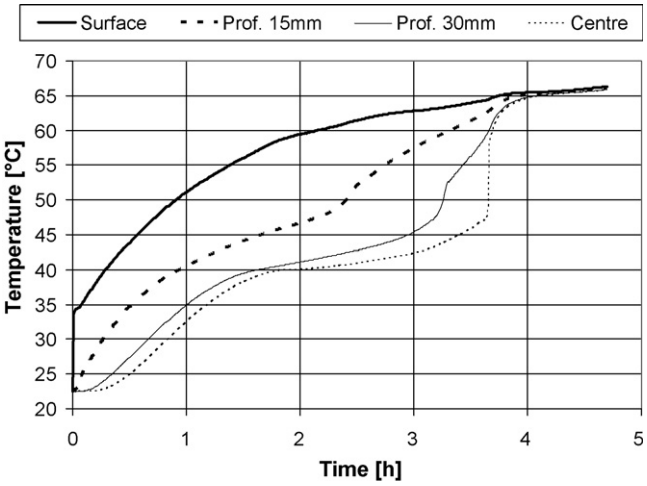

Fig. 16. Simulation taking into account internal convection inside PCM (80 nodes).

○ To a spherical cavity with: $10^2 < Ra < 10^9$ [7]

$$Nu = 0.228\,Ra^{0.226} \tag{16}$$

Fig. 15 shows results while taking into account the internal convection inside PCM. The small oscillations on the curves are generated by the non-continuity of the simulation model (meshing). It should be noticed that these oscillations have nothing to do with numerical instability. Between two spatial nodes, the change from solid to liquid is instantaneous for each layer depending on the temperature node. So, the effective conduction coefficient gets suddenly a strong variation between two time steps.

While increasing the node number for the PCM module calculations, it is possible to reduce the temperature oscillations as Fig. 16 shows due to a reduction of spatial meshing.

On the other hand, simulation time increases also strongly with the increase of the node number. In the example of Fig. 16, this simulation time is multiplied by a factor 30 for an increase of the calculation nodes of a factor 4 (20–80 nodes) as obtained in Fig. 15. In future studies, requiring yearly simulations, it will be necessary to limit the node number in order to reduce calculation time.

3. Conclusion

The simulation of the heat transfer between water and PCM module is often difficult to solve. Indeed, the internal convection inside PCM module is often disregarded to simplify the model. This approach is only foreseeable for PCM having a very big viscosity. For the other PCM, such as paraffin, it is necessary to take into account the internal convection. The model presented here, uses the effective conduction coefficient approach.

The comparison between monitored data and simulation results has shown a good agreement.

This method has an interesting potential and seem promising. However, it remains to confirm its qualities by performing other measurements and by reducing the

temperature oscillations observed when the phase change occurs, without increasing significantly the simulation time.

Acknowledgements

We would like to thank our national government (Federal Office of Energy (OFEN/BFE)). We also would like to deeply thank Jean-Christophe Hadorn, representative of the International Energy Agency (IEA) for having initiated the Task 32.

References

[1] J. Jokisalo, et al., Thermal Simulation of PCM Structures with TRNSYS Terrastock 2000, in: Proceedings of the Eighth International Conference on Thermal Energy Storage, Stuttgart, Germany, 2000.

[2] H. Visser, Energy storage in phase-change materials—development of a component model compatible with the TRNSYS transient simulation program, Delft University of Technology (1986).

[3] P. Egolf, Project Latentwärmespeicher für die Sonnenenergienutzung: Lade-und Entladevorgänge, EMPA-1997.

[4] S.A. Klein, TRNSYS reference manual http://sel.me.wisc.edu/trnsys.

[5] J. Bony et al., Three different approaches to simulate PCM bulk elements in solar storage tank, PCM2005, Yverdon-les-Bains, June 2005.

[6] F.P. Incropera, D.P. De Witt, Fundamentals of Heat and Mass Transfer (1990).

[7] Y.A. Cengel, Heat Transfer: A Practical Approach, International Edition 1997.

[8] E. Achenbach, Heat and flow characteristics of packed beds, Experimental Thermal and Fluid Science 10 (1995) 17–27.